Lab on a Chip

RSC Publishing

PAPER

View Article Online
View Journal | View Issue

Cite this: *Lab Chip*, 2013, **13**, 1394

Disaggregation of microparticle clusters by induced magnetic dipole–dipole repulsion near a surface†

Yang Gao,‡[a] Alexander van Reenen,‡[b] Martien A. Hulsen,[a] Arthur M. de Jong,[b] Menno W. J. Prins[bc] and Jaap M. J. den Toonder*[ac]

Received 6th November 2012,
Accepted 16th January 2013

DOI: 10.1039/c3lc41229f

www.rsc.org/loc

Ensembles of magnetic particles are known to align and aggregate into multi-particle clusters in an applied magnetic field, and the physical laws governing these processes are well described in literature. However, it has been elusive how to achieve the opposite process, *i.e.* the disaggregation of particle clusters in a magnetic field. We report a novel method to disaggregate clusters of superparamagnetic microparticles using time-dependent magnetic fields. The disaggregating field is designed to generate repulsive dipole–dipole forces between the particles and to stabilize the disaggregated particles on a physical surface. We demonstrate the disaggregation of large clusters of several tens of particles, within about one minute, using fields generated by a multipole electromagnet. After the disaggregation process the particles are uniformly distributed over the surface and ready for further lab-on-chip processing. Our results represent a novel methodology to disaggregate magnetic particle clusters and thereby improve the effectiveness and reproducibility of biological assays based on magnetic microparticles.

1 Introduction

Magnetic microparticles are being applied in many biochemical assays in order to capture, transport, separate, label, and mix the biological material.[1,2] Due to the high surface-to-volume ratio and the control over the surface properties, magnetic particles are very suitable for nucleic acid enrichment,[3] immunoassays[4] and cell capturing.[5] Moreover, the dynamic behavior of magnetic particles can be precisely controlled using applied magnetic fields, for example to perform buffer exchange washing steps,[6–8] rapid immunoassays,[9–13] or to achieve effective fluid mixing.[14–18]

When particles are magnetically manipulated, there is a natural tendency of the particles to form multi-particle clusters, *e.g.* chains or aggregates, caused by attractive magnetic forces. The clustering reduces the accessibility of the particles and thereby reduces the effectiveness and reproducibility of the assays. Furthermore, the clustering is often not easily reversed, because non-specific interactions can cause the particles to stick[19,20] and because the thermal motion of the particles is relatively slow.

In this paper we present a novel method to magnetically break up clusters of magnetic microparticles. The disaggregation principle is based on (i) the application of repelling magnetic dipole–dipole forces and (ii) the stabilization of the particles by attracting them onto a physical surface, as is sketched in Fig. 1. In short, groups of magnetic particle clusters are drawn to a physical surface by means of a field gradient. This phenomenon is termed as magnetophoresis and is explained by Jones.[21] A horizontal magnetic field is applied to optimize the parallel alignment of the clusters with the surface. Disaggregation and redispersion are initiated by means of magnetic dipole–dipole repulsion generated by a vertical magnetic field oriented orthogonal to the surface. We believe that the proposed magnetic actuation protocol has the potential to be beneficial for handling of functionalized magnetic particles in many microfluidic applications.

2 Theoretical considerations

In this section, we introduce the basic equations that can be used to approximately describe the repulsive behavior between the magnetic particles near a physical surface.

Given the superparamagnetic nature of the magnetic particles, we can assume that their magnetization is always parallel to the externally applied magnetic field. Thus, each magnetic particle is characterized by its induced magnetic dipole moment: $\mathbf{m} = V_p \chi_p \frac{\mathbf{B}}{\mu_0}$ where V_p is the volume of the suspended particles, χ_p the effective magnetic particle suscept-

[a]*Department of Mechanical Engineering, Eindhoven University of Technology, Eindhoven, The Netherlands. E-mail: j.m.j.d.toonder@tue.nl; Tel: +31 40 247 5081*
[b]*Department of Applied Physics, Eindhoven University of Technology, Eindhoven, The Netherlands*
[c]*Philips Research, Royal Philips Electronics, The Netherlands*

† Electronic supplementary information (ESI) available: Supplementary figures and movies. See DOI: 10.1039/c3lc41229f

‡ These authors contributed equally to this work.

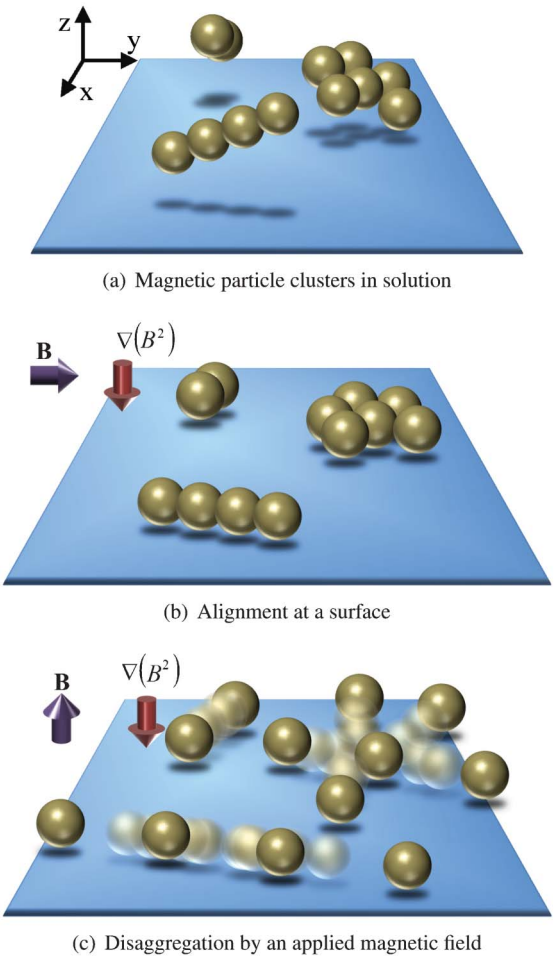

Fig. 1 Schematic disaggregation of magnetic particle clusters. (a) Clustered groups of magnetic particles are present in solution and (b) are drawn to a physical surface by means of a field gradient. A horizontal magnetic field is applied to optimize parallel alignment of the clusters with the surface. (c) Application of a vertical magnetic field oriented orthogonal to the surface in combination with a field gradient results in breaking of the particle clusters by magnetic dipole–dipole repulsion.

ibility, μ_0 the magnetic permeability of free space and **B** the applied magnetic flux density. The expression for the magnetic interaction force $\mathbf{F}^{\mathrm{mi}}{}_i$ between the i^{th} super-paramagnetic particle with the rest of the particles $(N-1)$ equals:[22,23]

$$\mathbf{F}_i^{\mathrm{mi}} = \frac{3\mu_0}{4\pi}\sum_{\substack{j=1\\ j\neq i}}^{N}\frac{m_i m_j}{r_{ij}^4}\left[(1-5(\hat{\mathbf{m}}\cdot\hat{\mathbf{r}}_{ij})^2)\hat{\mathbf{r}}_{ij}+2(\hat{\mathbf{m}}\cdot\hat{\mathbf{r}}_{ij})\hat{\mathbf{m}}\right] \quad (1)$$

where m_i is the strength of the dipole moment of the i^{th} particle, $\hat{\mathbf{m}}$ the unit vector of the magnetic field, r_{ij} the distance between the centers of the i^{th} and j^{th} particles and $\hat{\mathbf{r}}_{ij}$ the unit vector of the corresponding two particle chain axis.

If the particles are present in the same plane, a magnetic field oriented orthogonally to that plane will cause the dot product terms to vanish. This forces the magnetic interaction force $\mathbf{F}_i^{\mathrm{mi}}$ to be an outwardly directed force, driving/repelling the i^{th} particle away from the other particles.

To confine the particles at the same plane, magnetic field gradients are applied which move the corresponding particles to the nearby physical surface. The induced magnetic gradient force $\mathbf{F}_i^{\mathrm{mg}}$ acting on the i^{th} dipole is given as:[24]

$$\mathbf{F}_i^{\mathrm{mg}} = \frac{V_{\mathrm{p}}\chi_{\mathrm{p}}}{2\mu_0}\nabla B^2 \quad (2)$$

where B is the magnitude of the magnetic flux density. The combined use of a physical surface and a magnetic field gradient to bring and keep the particles there and an orthogonal oriented magnetic field is the key to separate superparamagnetic particle clusters and aggregates.

3 Experimental methods

3.1 Experimental system

A magnetic actuation setup was realized capable of manipulating suspended superparamagnetic particles triaxially, *i.e.* by generating a user-specified magnetic field both in the horizontal as well as in the vertical plane[25] (Fig. 2(a)). The setup consists of 8 individually controlled copper coils (brown) together with 8 soft-iron (ARMCO®) poles (dark grey) connected by soft-iron frames (blue and red). Magnetic fields are produced by the flow of electrical currents through the coils and by following the soft-iron frames, they are guided to the sample area surrounded by the poles. The blue soft-iron frames with 4 poles at their ends are used for the generation of the horizontal components of the magnetic field whereas the red frames are responsible for the vertical ones.

A closer view of sample area is given in Fig. 2(b). Here, each copper coil is numerically assigned and the sample area is positioned at the origin of the Cartesian coordinates. At the center of the sample area, a closed fluid cell is placed that contains a suspension of magnetic particles. The fluid cell has a diameter of 9 mm and a depth of 120 μm and is made using glass substrates and Secure-Seal spacers (Grace BIO-LABS®). During each experiment (T = 293 K), the suspended magnetic particles are actuated using the magnetic setup and the resulting dynamics are analyzed using video-microscopy.

We chose to work with polymer-based superparamagnetic particles (2.8 μm) coated with streptavidin (Dynabeads® M-270 Streptavidin). Due to the high binding affinity of the streptavidin–biotin interaction, streptavidin-coupled Dynabeads have been utilized in a vast number of applications, *e.g.* isolation and handling of biotinylated nucleic acids, antibodies and other biotinylated ligands and targets. The undiluted stock suspension was diluted 10 times (6.5×10^7 particles/ml) using a buffer solution (PBS + 1 mg ml^{-1} BSA) before introducing into the fluid cell. The magnetic properties of the particles were characterized using VSM.

3.2 Characterization of the setup

The possibility of generating arbitrary magnetic fields using the setup was investigated by modeling the setup in a 3D commercial FEM package (Comsol Multiphysics®). In Fig. S1(a),† the modeled setup including 8 individually controlled coils is depicted. The soft-iron and copper materials were

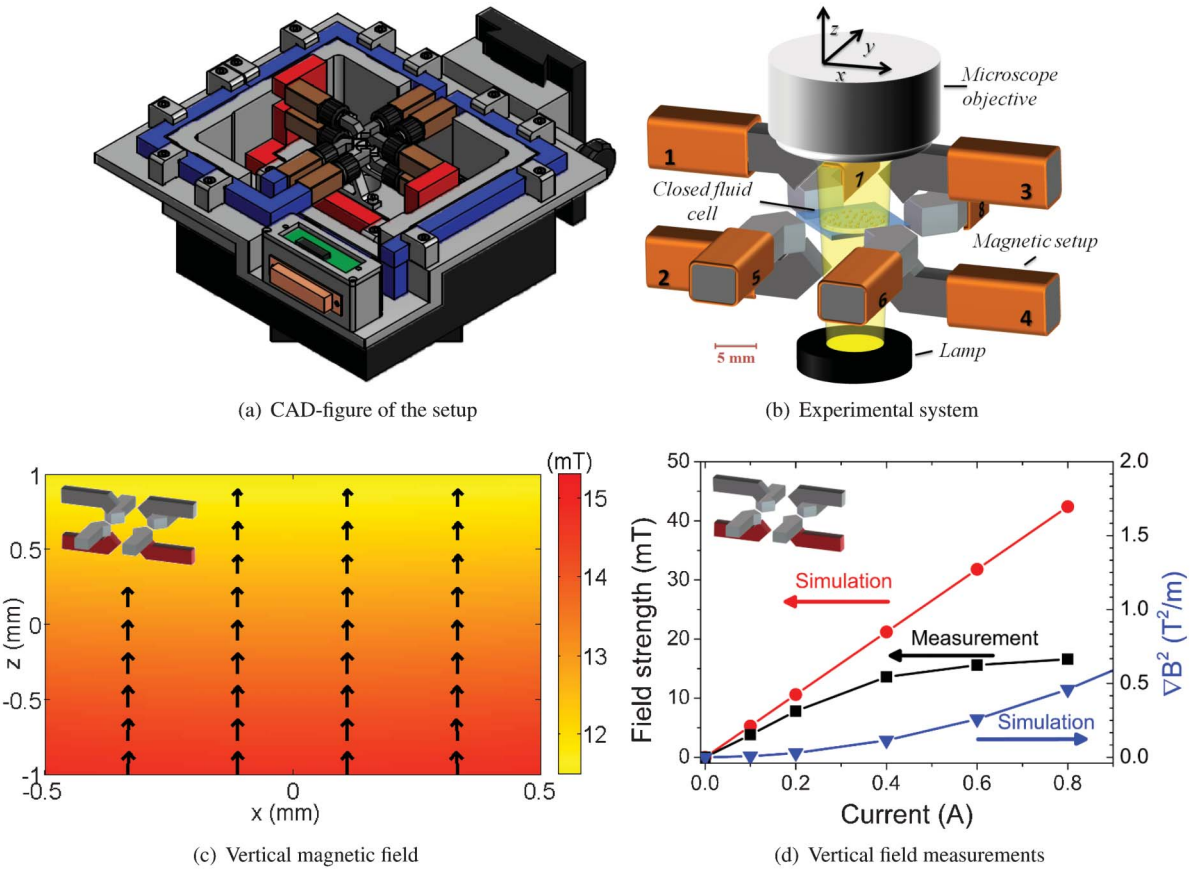

Fig. 2 3D magnetic actuation setup. (a) AutoCAD side-view of the set-up. (b) The magnetic setup with the fluid cell at the center under a microscope. (c) Simulated vertical magnetic field induced by coils 2 and 4 at a current of 0.25 A. (d) (left *y*-axis): Experimental measurements of the magnitude of the vertical magnetic field are compared with results from Comsol simulations. (d) (right *y*-axis): Generated field gradient in the center of the setup as obtained from Comsol simulations. The vertical magnetic field of coils 2 and 4 induces a field gradient in the $-e_z$ direction.

modeled as linear media with relative permeabilities (μ_r) of 4750 and 1, respectively.

In the experiments we report in this paper, we generated three particular magnetic fields: (1) a vertical field with a downward gradient by flowing currents through coils 2 and 4 simultaneously, (2) a uniform horizontal field by running currents through coils 5 and 8 and (3) a horizontally rotating field, which is created by applying currents to coils 5 to 8 that vary sinusoidally in time, and have a phase shift of 90 degrees between them. Fig. 2(c) shows the computed magnetic field in the *z*–*x* (vertical) plane, generated by the flow of opposing electrical currents (0.25 A) through coils 2 and 4. As expected, the magnitude of the vertical field shows a decrease along the *z*-axis. In contrast, coils 5 and 8 (0.2 A) induce a more homogenous magnetic field in the horizontal (*y*–*x*) plane (Fig. S1(b)†).

The setup was experimentally characterized by measuring the magnitudes of the generated magnetic fields as depicted in Fig. 2(c) and S1(b)† using a Gauss meter (F.W. Bell®). The measurements took place at the center of the setup and the electrical currents through the coils were varied from 0.1 to 1 A. The experimentally measured values were compared with results from Comsol simulations.

The results are shown at the left *y*-axes of Fig. 2(d) and S1(c).† It is seen that saturation of the magnetic fields occurs at electrical currents higher than 0.4 A, and below this value the experiments and computations show linear trends. The observed difference between the simulation and experiment shows that the soft-iron used in the magnetic set-up has non-linear material properties, leading to saturation of the induced magnetic field, which is not included in the numerical simulations. In the present study, experiments were conducted at a limiting electrical current of 0.5 A as higher currents do not yield a higher magnetic field strength.

The geometry of the set-up is designed in such a way that electrical currents through coils 2 and 4 (Fig. 2(c)) generate in addition magnetic field gradients towards the corresponding poles, whereas this is not the case when coils 5 and 8 are operational (Fig. S1(b)†). Here, magnetic field gradients are defined as the gradients of the modulus of magnetic flux density (**B**) to the square. At the right *y*-axes of Fig. 2(d) and S1(c),† simulated field gradients are plotted for the vertical and horizontal configurations. On the one hand, coils 2 and 4 generate vertical magnetic field gradients, pulling the suspended magnetic particles to the substrate. On the other hand,

coils 5 and 8 induce a homogeneous magnetic field in the horizontal plane.

4 Results and discussion

In the current study, we explore the possibility of manipulating a collection of sedimented superparamagnetic particles in a fluid cell, using magnetic actuation protocols. In particular, we are interested in the influence of the vertical magnetic field (Fig. 2(c)). If the particles are present in the same horizontal plane, applying a vertically oriented magnetic field will cause mutual repulsion between the particles, which have become vertically oriented magnetic dipoles in the horizontal plane.

Specifically, if coils 2 and 4 are actuated with a current of 0.4 A, the corresponding magnetic field and gradient (Fig. 2(d)) acting on the particles are equal to 13.6 mT and 0.1148 $T^2\ m^{-1}$, respectively. Referring to eqn (1) and (2), the generated repulsive and gradient forces on a dipole–dipole cluster are strong and are equal to ~22 pN and ~0.3 pN.

This phenomenon can be exploited in a number of ways as we will see below: it offers the possibility to control the distribution of sedimented magnetic particles and when combining with the ability to generate horizontal fields intermittent to vertical fields, it provides a new way to de-cluster unwanted formation of particle clusters and aggregates.

4.1 Initialization of particle distribution

Fig. 3(a) shows the initial magnetic particle distribution (t = 0 s) after a suspension of magnetic particles was introduced into the fluid chamber and the particles were allowed to sediment to the bottom substrate, *i.e.* the floor of the fluid chamber. Here, no external magnetic field was applied. The sedimented magnetic particles form a random distribution over the surface and due to the presence of a small remnant magnetic field (⩽1 mT), cluster formation of the magnetic particles is observed. This initial distribution of the magnetic particles is difficult to control and varies per experiment. However, in order to obtain experimentally repeatable and reproducible data, it is important to have a controllable and fixed initial condition of the magnetic particles.

Fig. 3(b) shows the resulting configuration of the magnetic particles after applying a vertical magnetic field (14.6 mT, 12 s). The magnetic field was generated by the flow of opposing electrical currents (0.5 A) through coils 2 and 4. As we have seen in Fig. 2(d), also vertical magnetic field gradients were generated which pulled the magnetic particles to the chamber floor. Due to the vertical magnetic field, the sedimented magnetic particles mutually repelled each other until a relatively uniform configuration was formed which approximately resembles a hexagonal lattice structure. Video microscopy results corresponding to the particle distribution initialization process can be found in Mov1.†

In Fig. 3(c), the nearest particle–neighbor distance (obtained from video-microscopy results above) is plotted against the actuation time. Here, the nearest neighbor distance is calculated by averaging the nearest neighbor distances

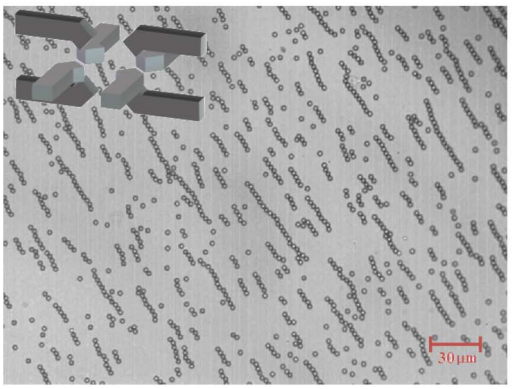

(a) Initial magnetic particle distribution

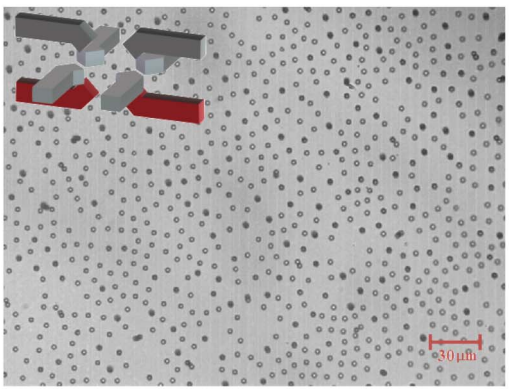

(b) Magnetic particle distribution in $\mathbf{B} = B\mathbf{e}_z$

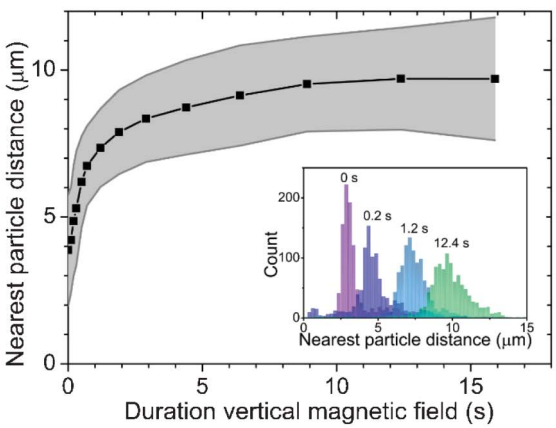

(c) Nearest particle-neighbor distance

Fig. 3 Controlling magnetic particle distribution using a vertical magnetic field (14.6 mT). (a) Initial magnetic particle distribution as the particles were introduced into the fluid chamber and allowed to sediment on the surface (t = 0 s). (b) After applying a vertical magnetic field, sedimented magnetic particles become vertically oriented dipoles and mutually repel each other (t = 12 s). (c) The average nearest neighbor distance calculated from ~1000 particles is plotted against the field duration. The grey area indicates the corresponding standard deviation. The inset shows distributions of the nearest neighbor distances plotted at 4 different field durations.

surrounding ~1000 particles with the grey area as the corresponding standard deviation. The slope of the graph shows an exponential decay which can be attributed to the

generated repulsive force (eqn (1)), *i.e.* it is a short-range force as it is inversely dependent on the inter-particle distance to the fourth power. Eventually, the particles mutually repel each other, forming an approximately hexagonal lattice structure with an average inter-particle distance of $\sim$10 μm.

From these results, it is clear that by controlling the initial concentration of the magnetic particle suspension along with the magnitude of the vertical magnetic field and its gradient, the magnetic particle distribution at the beginning of every experiment can be controlled and fixed to an almost uniform distribution.

4.2 Overcoming non-specific interparticle adhesion

Besides successful separation of particles (Fig. 3), we also observe that a small fraction of particles is still present as chains aligned in the applied (vertical) field direction. We can distinguish two different ways of obtaining such vertical chains. On the one hand, thermal fluctuations of individual particles can cause the particles to move out of the horizontal plane. As a result, the lifted particles can make a transition from the weakly stable state of parallel alignment to the surface (in-plane) to the more stable state of orthogonal alignment to the surface (out-of-plane). This in-plane to out-of-plane rearrangement process is enhanced by a roughness of the physical surface and/or the particles. The in-plane stability of the particles can be enhanced by using stronger field gradients or larger particles.

On the other hand, we also observe that a few clusters realign to the applied vertical field without any observable separation of the particles. This behavior may be attributed to non-specific interactions that keep the particles stuck to each other. Non-specific interactions may originate from van der Waals forces or electrostatic forces for example. When magnetic fields are used to control magnetic particles, the attractive forces acting on the particles are typically on the order of 10 pN (according to eqn (1)). Such forces ensure that the particles come into close contact and promote attractive non-specific interactions. This is important for particles functionalized with proteins, as in our experiments, because protein-coated particles can have a weak surface charge and contain non-polar (= hydrophobic) regions.

It is interesting to estimate whether it is possible to rupture non-specific bonds. We calculate (using eqn (1)) that the repulsive dipole–dipole forces which we apply to our particles are in the order of 22 pN ''for a flux density in the order of 14 mT''. Furthermore, we observe that two-particle clusters which do not separate, realign with the magnetic field within 0.1–0.2 s. In order to dissociate such bonds, not only the force is important, but also the time during which the force is applied. A previous study on the breaking of non-specific bonds between magnetic particles and a substrate in the presence of surfactants[19] has shown that a force of 1.2 pN needs to be applied for $\sim$2 s to disrupt the weak non-specific bonds. The dissociation constant could be estimated to be 0.83 s^{-1} at a force of 1.2 pN.

At the same force, the method presented here would result in a dissociated fraction, *i.e.* the amount of non-specific bonds being ruptured for two particles clusters, of roughly $\sim$0.1. However, we apply a force that is almost 20 times higher. This would definitely lead to a higher dissociated fraction as estimated here. Moreover, dissociation can still be enhanced by increasing the field gradient or by saturating the magnetic moment. Respectively, this would make the application time longer and increase the strength of the repulsive forces. Therefore, we conclude that the repelling forces exerted using the method presented in this paper are in a force regime which can rupture non-specific bonds.

4.3 Controlled clustering and disaggregation of particles

Vertical (14.6 mT) and horizontal (13.7 mT) magnetic fields are utilized to break and reform large aggregates of magnetic particles. A horizontal rotating magnetic field (13.7 mT, 0.5 Hz) was used to form such structures.

Initially, sedimented magnetic particles (Fig. 4(a)) form chains that rotate along with the magnetic field (Fig. 4(b)). Rotating chain dynamics have been suggested[9,15] to enhance fluids mixing and selective binding between the functionalized magnetic particles with the target biomarkers. After 4 rotating cycles (Fig. 4(c)), clusters and aggregates appear that drastically reduce the available binding surface of the coated magnetic particles. Active breaking of the clusters is necessary, since particles remain in their aggregated form due to non-specific interactions even when the magnetic field has been turned off.

To break down the formed clusters, a magnetic actuation protocol is executed consisting of applying, alternately, vertical and horizontal components of the magnetic field. The vertical magnetic field acts to break down clusters when they are aligned with the bottom substrate (the horizontal plane). In Fig. 4(d), the breaking of horizontal clusters is depicted. As can be seen, some parts of the broken clusters align with the vertical magnetic field, forming vertical clusters. A horizontal magnetic field is then used to realign the vertical clusters with the bottom substrate (Fig. 4(e)).

In a similar way, alternating vertical and horizontal magnetic fields are applied sequentially to break down the remaining clusters. The frequency of switching between the two states is 5 Hz. At the end of the de-cluster protocol (50 s), the resulting bead suspension is homogenously dispersed over the substrate surface (Fig. 4(f)). After this, a rotating magnetic field can be applied again to form rotating magnetic particle chains and restart the whole process. Video-microscopy results corresponding to the controlled clustering and disaggregation of particles can be found in Mov2.†

Video-microscopy results from the de-cluster experiment were analyzed using computer software (ImageJ) and the results are shown in Fig. 5. Here, we define both unclustered particles and particle aggregates as individual entities. The total amount of the entities and the average amount of particles per entity are counted and plotted against time (Fig. 5(a)). The corresponding shaded areas represent the error related to the Poisson distribution. In agreement with Fig. 4, at the beginning of the experiment (t = 0 s), the average amount of particles per entity is low and the amount of entities is high. As many rotating particle chains cluster into few rotating clusters, the average entity size reaches a peak ($t \leqslant 10$ s). After applying the breaking protocol (starting at $t > 10$ s), both

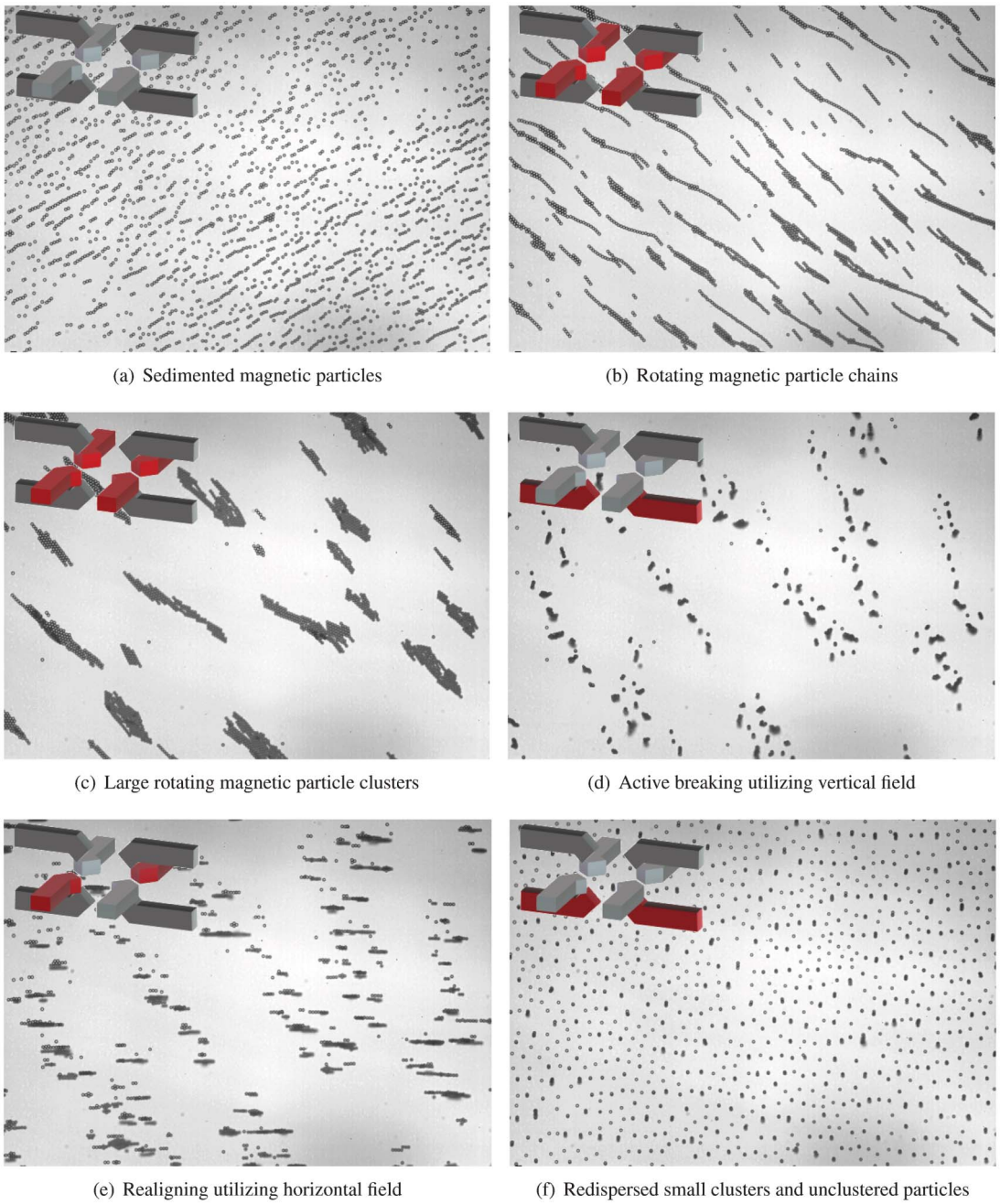

Fig. 4 Magnetic actuation protocol to disaggregate particle clusters. (a) Initial distribution of the sedimented magnetic particles. (b) Rotating magnetic particle chains are formed with field strength equals 13.7 mT and rotational frequency equals 0.5 Hz. (c) Large rotating clusters of magnetic particles are formed. (d) Vertical magnetic field (14.6 mT) is used to break the horizontally aligned clusters. (e) Horizontal magnetic field (13.7 mT) is applied to realign the vertical clusters with the surface. (f) At the end of the protocol (50 s), the suspension is homogenously distributed over the physical surface.

quantities return to the states similar to the beginning of the experiment.

In a similar way, Fig. 5(b) shows the fraction of unclustered particles during the experiment. For $t \leqslant 10$ s, this decreases from 0.4 to 0 due to the formation of large particle aggregates. After starting the disaggregation protocol, the fraction of unclustered particles climbs up to a value around 0.3 which indicates a regeneration performance of 75% within 50 s.

We believe that the proposed magnetic actuation protocol is a new way to remove unwanted clusters and aggregates of magnetic micro-particles (some aggregates even containing 60 particles) and to regenerate the magnetic particle distribution to a uniform state so that one sample of magnetic particles can be used multiple times to catch the seeded target bio-molecules.

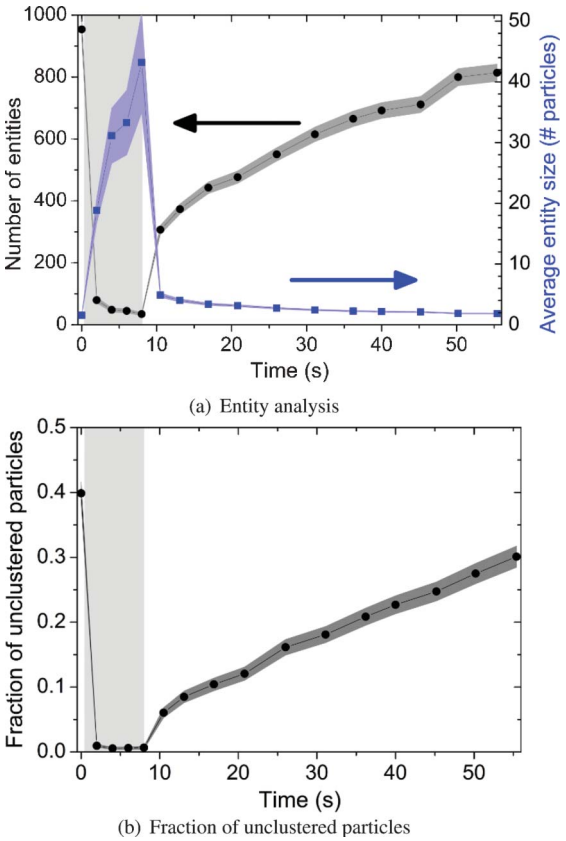

Fig. 5 Particle analysis of the disaggregation experiment. The light grey areas indicate the period of cluster formation. The dark shaded areas indicate the error related to the Poisson distribution. (a) The total amount of entities (left *y*-axis) and the average amount of particles per entity (right *y*-axis) are plotted against time. Here, we define both unclustered particles and particle aggregates as entities. (b) The fraction of unclustered particles is plotted against time.

5 Conclusion

We have demonstrated a method to disaggregate clusters of magnetic particles by applied magnetic fields. The particle clusters are attracted to a physical surface by a magnetic field gradient and broken up by an orthogonally oriented magnetic field which induces repulsive dipole–dipole interactions between the clustered particles. As a result, non-specific adhesion between the particles can be overcome and the particles are uniformly distributed over the surface. For small particle clusters of less than 10 particles, a single application of this method is sufficient to almost fully redisperse the particles. Larger particle clusters up to 60 particles can be almost completely redispersed by repeated application of the field configuration, interleaved with the application of a weaker in-plane field to reorient the remaining clusters.

The disaggregation technique will open new possibilities for lab-on-a-chip processes based on magnetic particles. An advantage is that a uniform particle configuration can be reestablished during the assay. A reset of the particle distribution can be very useful for magnetically actuated fluid mixing procedures[14–18] and target capture procedures[9,10] in microfluidic systems, as a high mixing and capture efficiency can be maintained by disaggregating clusters during the actuation processes.

Furthermore, the disaggregation method can be used to reduce non-specific adhesion between the particles. The results presented in this paper have been obtained with streptavidin-functionalized particles dispersed in a physiological buffer with blocking proteins. The weak surface charge of the particles and the high ionic strength of the buffer cause weak repulsive electrostatic interactions between the particles, and thereby enable the occurrence of non-specific inter-particle bonds in the experiments. The disaggregation method of this paper was able to rupture the non-specifically bound clusters of particles and to thereby regenerate unbound particles. In follow-up research, it will be interesting to further study the biological window of operation of the disaggregation method for different particle types, and to evaluate which fields and field gradients are needed to break non-specific binding in fluids of increasing biological complexity. In addition, it will be interesting to study the case of extremely high particle concentrations, in which large particle aggregates will be formed that need to be redistributed uniformly over the surface. This can be done by applying a horizontal field gradient in combination with the proposed de-clustering protocol.

In summary, we have presented a novel technique to disaggregate clusters of magnetic particles. The technique will increase the effectiveness and reproducibility of magnetic particle based biological assays and will enlarge the application range of magnetic particles in lab-on-a-chip devices.

Acknowledgements

We gratefully acknowledge the engineers at EPC (TU Eindhoven) for manufacturing the setup. This work was supported by Technology Foundation STW under grant 10458.

References

1 M. A. M. Gijs, *Microfluid. Nanofluid.*, 2004, **1**, 22–40.
2 N. Pamme, *Lab Chip*, 2006, **6**, 24–38.
3 *The Nucleic Acid Protocols Handbook*, ed. R. Rapley, Humana Press, 2000.
4 *The Immunoassay Handbook*, ed. D. Wild, Gulf Professional Publishing, 2005.
5 D. J. Sherman, V. E. Kenanova, E. J. Lepin, K. E. McCabe, K. Kamei, M. Ohashi, S. Wang, H. Tseng, A. M. Wu and C. P. Behrenbruch, *Anal. Biochem.*, 2010, **401**, 173–181.
6 J. Nam, C. S. Thaxton and C. A. Mirkin, *Science*, 2003, **301**, 1884–1886.
7 Z. Chen, S. M. Tabakman, A. P. Goodwin, M. G. Kattah, D. Daranciang, X. Wang, G. Zhang, X. Li, Z. Liu, P. J. Utz, K. Jiang, S. Fan and H. Dai, *Nat. Biotechnol.*, 2008, **26**, 1285–1292.
8 S. J. Osterfeld, H. Yu, R. S. Gaster, S. Caramuta, L. Xu, S. Han, D. A. Hall, R. J. Wilson, S. Sun, R. L. White, R.

W. Davis, N. Pourmand and S. X. Wang, *Proc. Natl. Acad. Sci. U. S. A.*, 2008, **105**, 20637–20640.
9 K. Tanaka and H. Imagawa, *Talanta*, 2005, **68**, 437–441.
10 Y. Moser, T. Lehnert and M. A. M. Gijs, *Lab Chip*, 2009, **9**, 3261–3267.
11 D. M. Bruls, T. H. Evers, J. A. H. Kahlman, P. J. W. van Lankvelt, M. Ovsyanko, E. G. M. Pelssers, J. J. H. B. Schleipen, F. K. de Theije, C. A. Verschuren, T. van der Wijk, J. B. A. van Zon, W. U. Dittmer, A. H. J. Immink, J. H. Nieuwenhuis and M. W. J. Prins, *Lab Chip*, 2009, **9**, 3504–3510.
12 A. Ranzoni, X. J. A. Janssen, M. Ovsyanko, L. J. van IJzendoorn and M. W. J. Prins, *Lab Chip*, 2010, **10**, 179–188.
13 A. Ranzoni, J. J. Schleipen, L. J. van IJzendoorn and M. W. J. Prins, *Nano Lett.*, 2011, **11**, 2017–2022.
14 S. L. Biswal and A. P. Gast, *Anal. Chem.*, 2004, **76**, 6448–6455.
15 T. G. Kang, M. A. Hulsen, P. D. Anderson, J. M. J. den Toonder and H. E. H. Meijer, *Phys. Rev. E*, 2007, **76**, 066303.
16 S. H. Lee, D. v. Noort, J. Y. Lee, B. Zhang and T. H. Park, *Lab Chip*, 2009, **9**, 479–482.
17 T. Franke, L. Schmid, D. A. Weitz and A. Wixforth, *Lab Chip*, 2009, **9**, 2831–2835.
18 T. Roy, A. Sinha, S. Chakraborty, R. Ganguly and I. K. Puri, *Phys. Fluids*, 2009, **21**, 027101.
19 S. Upadhyayula, T. Quinata, S. Bishop, S. Gupta, N. R. Johnson, B. Bahmani, K. Bozhilov, J. Stubbs, P. Jreij, P. Nallagatla and V. I. Vullev, *Langmuir*, 2012, **28**, 5059–5069.
20 M. Kemper, D. Spridon, L. J. van IJzendoorn and M. W. J. Prins, *Langmuir*, 2012, **28**, 8149–8155.
21 T. B. Jones, *Electromechanics of Particles*, Cambridge University Press, New York City, NY, 1995.
22 S. Melle, O. G. Caldern, M. A. Rubio and G. G. Fuller, *Phys. Rev. E*, 2003, **68**, 041503.
23 S. Krishnamurthy, A. Yadav, P. Phelan, R. Calhoun, A. Vuppu, A. Garcia and M. Hayes, *Microfluid. Nanofluid.*, 2008, **5**, 33–41.
24 R. J. S. Derks, A. Dietzel, R. Wimberger-Friedl and M. W. J. Prins, *Microfluid. Nanofluid.*, 2007, **3**, 141–149.
25 Y. Gao, M. A. Hulsen, T. G. Kang and J. M. J. den Toonder, *Phys. Rev. E*, 2012, **86**, 041503.